Global phase diagram for magnetism and lattice distortion of iron-pnictide materials

Yang Qi and Cenke Xu
Department of Physics, Harvard University, Cambridge, Massachusetts 02138, USA
(Received 9 January 2009; revised manuscript received 2 August 2009; published 4 September 2009)

We study the global phase diagram of magnetic orders and lattice structure in the Fe-pnictide materials at zero temperature within one unified theory tuned by both electron doping and pressure. On the low doping and high-pressure side of the phase diagram, there is one single transition, which is described by a $z=2$ mean-field theory with very weak run-away flows; on the high doping and low-pressure side, the transition is expected to split to two transitions, with one O(3) spin-density wave transition followed by a $z=3$ quantum Ising transition at larger doping. The fluctuation of the strain field of the lattice will not affect the spin-density wave transition but will likely drive the Ising nematic order transition a mean-field transition through a linear coupling, as observed experimentally in $BaFe_{2-x}Co_xAs_2$.

DOI: 10.1103/PhysRevB.80.094402 PACS number(s): 73.43.Nq, 75.30.Fv, 74.25.Dw

I. INTRODUCTION

The iron superconductor, for its potential to shed new light on the non-BCS type of superconductors, has attracted enormous interests since early this year. Despite the complexities and controversies on the superconducting mechanism, the minimal tight-binding model, or even the exact pairing symmetry of the cooper pair, these samples do share two common facts: the tetragonal-orthorhombic lattice distortion and the $(\pi,0)$ spin-density wave (SDW).[1] Both effects are suppressed under doping and pressure, and they seem always to track each other in the phase diagram. In Refs. 2 and 3, the lattice distortion is attributed to preformed spatially anisotropic spin correlation between electrons, without developing long-range SDW, i.e., the lattice distortion and SDW both stem from magnetic interactions. More specifically, the Ising order parameter σ, which drives the orthorhombic lattice distortion, is represented as $\sigma=\vec{\phi}_1\cdot\vec{\phi}_2$, $\vec{\phi}_1$, and $\vec{\phi}_2$ are two Neel orders on the two different sublattices of the square lattice.

Since this order deforms the electron Fermi surface, equivalently, it can also be interpreted as electronic nematic order. The intimate relation between the structure distortion and SDW phase has gained many supports from recent experiments. It is suggested by detailed x-ray, neutron, and Mössbauer spectroscopy studies that both the lattice distortion transition and the SDW transition of $LaFeAs(O_{1-x}F_x)$ are second order,[4] where the two transitions occur separately. However, in undoped AFe_2As_2 with $A=Sr,Eu,Ba,Ca$, the structure distortion and SDW occur at the same temperature, and the transition becomes a strong first-order transition.[5–9] Also, recent neutron-scattering measurements on $Fe_{1+y}Se_xTe_{1-x}$ indicate that in this material the SDW wave vector is $(\pi/2,\pi/2)$ for both sublattices[10] instead of $(\pi,0)$, as in 1111 and 122 materials, and the low-temperature lattice structure is monoclinic instead of orthorhombic (choosing one-Fe unit cell). These results suggest that the SDW and structure distortion are indeed strongly interacting with each other and, probably, have the same origin. The sensitivity of the location of the lattice distortion transition close to the quantum critical point against the external magnetic field (magnetoelastic effect) can further confirm this unified picture.

The clear difference between the phase diagrams of 1111 and 122 materials can be naturally understood in the unified theory proposed in Refs. 2 and 3. We can write down a general Ginzburg-Landau mean-field theory for σ, $\vec{\phi}_1$, and ϕ_2,

$$F_{GL}=(\nabla_\mu\sigma)^2+r_\sigma\sigma^2+\sum_{a=1}^{2}(\nabla_\mu\vec{\phi}_a)^2+r_\phi|\vec{\phi}_a|^2+\tilde{u}\sigma\vec{\phi}_1\cdot\vec{\phi}_2+\cdots. \quad (1)$$

r_σ and r_ϕ are tuned by the temperature. For a purely two-dimensional system, the Ising order, which induces the lattice distortion, occurs at a temperature controlled by the in-plane spin coupling $T_{Ising}\sim J_{in}$,[11] while there is no SDW transition at finite temperature; for weakly coupled two-dimensional layers, the Ising transition temperature is still controlled by the in-plane coupling, while the SDW transition temperature is $T_{sdw}\sim J_{in}/\ln(J_{in}/J_z)$, with $J_z\ll J_{in}$ representing the interlayer coupling. This implies that on quasi-two-dimensional lattices $T_{Ising}\geq T_{sdw}$ or $\Delta r=r_\phi-r_\sigma$ is large in the Ginzburg-Landau mean-field free energy in Eq. (1). In real systems, the 1111 materials are much more anisotropic compared with the 122 materials since the electron band structure calculated from local-density approximation (LDA) shows a much weaker z direction dispersion compared with the 122 samples;[12] also the upper critical field H_{c2} of 122 samples is much more isotropic.[13] This justifies treating the 1111 materials as a quasi-two-dimensional system, while treating the 122 materials as a three-dimensional (3D) one. When J_z and J_{in} are close enough, Δr is small and the interaction between the Ising order parameter and the SDW will drive the transition first order by minimizing the free-energy Eq. (1). The phase diagram of free-energy Eq. (1) is shown in Fig. 1.

Motivated by more and more evidences of quantum critical points in the Fe-pnictides superconductors,[14–19] in this work, we will explore the global phase diagram of magnetic and nematic orders at zero temperature tuned by two parameters: pressure and doping. In Sec. II we will study the phase diagram for quasi-two-dimensional lattices, with applications for 1111 materials, and in Sec. III the gear will be switched

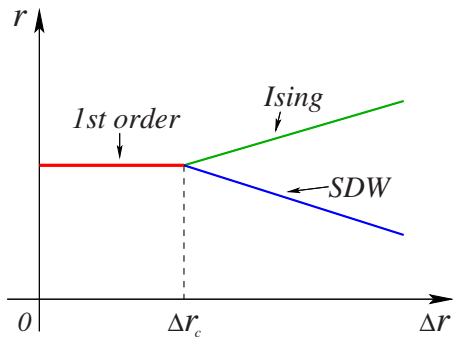

FIG. 1. (Color online) The schematic phase diagram of Ginzburg-Landau mean-field theory in Eq. (1) plotted against $r=r_\sigma+r_\phi$ and $\Delta r=r_\phi-r_\sigma$. r is linear with temperature T, while Δr is tuned by anisotropy ratio J_z/J_{in}. When Δr is small, the interaction between $\vec{\phi}_1$ and $\vec{\phi}_2$ induces a strong first-order transition, which corresponds to the undoped 122 materials with more isotropic electron kinetics; when Δr is large, the transition is split into two transitions, with an Ising transition followed by an SDW transition at lower temperature, and this is the case in the 1111 materials with quasi-two-dimensional dispersions. The multicritical point Δr_c is determined by $\tilde{u}$.

to the more isotropic $3d$ lattices of 122 materials. Section IV will briefly discuss the effect of the coupling between the Ising transition and the strain tensor of the lattice, which will drive the finite temperature Ising nematic transition a mean-field transition, while the SDW transition remains unaffected, as observed in $BaFe_{2-x}Co_xAs_2$.[17] The analyses in our current work are all only based on the symmetry of the system and, hence, independent of the details of the microscopic model.

II. QUASI-TWO-DIMENSIONAL LATTICE

In Ref. 2, the zero-temperature quantum phase transition was studied for weakly coupled $2d$ layers with finite electron doping. Since the hole pockets and the electron pockets have small and almost equal size, the slight electron doping would change the relative size of the electron and hole pockets substantially. Also, the neutron-scattering measurement suggests that the SDW order wave vector is independent of doping in 1111 materials.[14] Therefore, under doping the low-energy particle-hole pair excitations at wave vector $(\pi,0)$ are lost very rapidly, and the spin-density wave order parameter at low frequency and long-wavelength limit can no longer decay with particle-hole pairs (the fermi pockets are schematically showed in Fig. 2). After integrating out electrons, we would obtain the following $z=1$ Lagrangian:[2]

$$L=\sum_{i=1}^{2}\sum_{\mu=\tau,x,y}\partial_\mu\vec{\phi}_i\cdot\partial_\mu\vec{\phi}_i-r\vec{\phi}_i^2+u|\vec{\phi}_i|^4+L',$$

$$L'=\gamma\vec{\phi}_1(\partial_x^2-\partial_y^2)\cdot\vec{\phi}_2+\gamma_1|\vec{\phi}_1|^2|\vec{\phi}_2|^2-\alpha(\vec{\phi}_1\cdot\vec{\phi}_2)^2, \quad (2)$$

which contains no damping term. The first three terms of the Lagrangian describe the two copies of 3D O(3) Neel orders on the two sublattices. The α term is the only relevant term at the 3D O(3) transition since it has positive scaling dimension $\Delta[\alpha]=0.581$.[20] We expect this term to split the two coinciding O(3) transitions into two transitions: an O(3) transition and an Ising transition for Ising variable $\sigma=\vec{\phi}_1\cdot\vec{\phi}_2$, as observed experimentally in 1111 materials.[14]

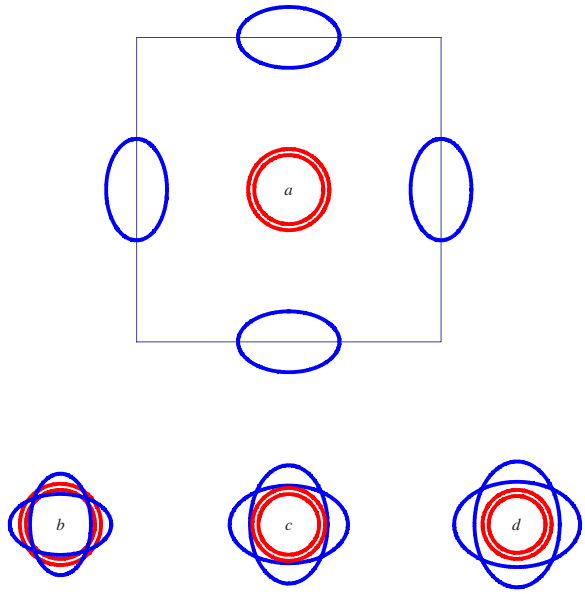

FIG. 2. (Color online) (a) The schematic two-dimensional Fermi pockets of 1111 materials, the concentric circles are two very close hole pockets, the ovals are electron pockets. (b) and (d) The relative position of hole and electron pockets after translating by $(\pi,0)$ and $(0,\pi)$ in the momentum space, in the low doping, critical doping, and high doping regimes.

The two transitions after splitting are an O(3) transition and an Ising transition. The O(3) transition belongs to the 3D O(3) universality class, while the Ising transition is a $z=3$, $d=2$ mean-field transition. This is because the Ising order parameter does not double the unit cell and, hence, can decay into particle-hole pairs at momentum (0,0). The standard Hertz-Millis theory[21] would lead to a $z=3$ mean-field transition.[2,22]

Now let us turn on another axis in the phase diagram: the pressure. Under pressure, the relative size of hole and electron pockets are not expected to change. Therefore, under translation of $\vec{Q}=(\pi,0)$ in the momentum space, the hole pocket will intersect with the electron pocket [Fig. 2(b)], which leads to overdamping of the order parameters. The decay rate can be calculated using Fermi's Golden rule,

$$\mathrm{Im}[\chi(\omega,q)]\sim\int\frac{d^2k}{(2\pi)^2}[f(\epsilon_{k+q})-f(\epsilon_{k+\vec{Q}})]\delta(\omega-\epsilon_{k+q}+\epsilon_{k+\vec{Q}})$$
$$\times|\langle k+Q|\vec{\phi}_{i,q}|k+q\rangle|^2\sim c_0\frac{\omega}{|\vec{v}_h\times\vec{v}_e|}. \quad (3)$$

v_h and v_e are the Fermi velocity at the points on the hole and electron pockets, which are connected by wave vector $(\pi,0)$. The standard Hertz-Millis[21] formalism leads to a coupled $z=2$ theory in the Euclidean momentum space with Lagrangian,

$$L_q = \sum_{i=1}^{2} \vec{\phi}_i \cdot (|\omega| + q^2 + r)\vec{\phi}_i + \gamma\vec{\phi}_1(q_x^2 - q_y^2) \cdot \vec{\phi}_2 + L',$$

$$L' = \tilde{A}(|\vec{\phi}_1|^4 + |\vec{\phi}_2|^4) - \alpha(\vec{\phi}_1 \cdot \vec{\phi}_2)^2 + \tilde{C}|\vec{\phi}_1|^2|\vec{\phi}_2|^2. \quad (4)$$

The parameter r can be tuned by the pressure. The Ising symmetry of $\sigma = \vec{\phi}_1 \cdot \vec{\phi}_2$ on this system corresponds to transformation

$$x \to y, \quad y \to x,$$

$$\vec{\phi}_1 \to \vec{\phi}_1, \quad \vec{\phi}_2 \to -\vec{\phi}_2, \quad \sigma \to -\sigma. \quad (5)$$

This Ising symmetry forbids the existence of term $\vec{\phi}_1 \cdot \vec{\phi}_2$ in the Lagrangian, while the mixing term $\gamma\vec{\phi}_1(q_x^2 - q_y^2) \cdot \vec{\phi}_2$ is allowed.

We can diagonalize the quadratic part of this Lagrangian by defining $\vec{\phi}_A = (\vec{\phi}_1 + \vec{\phi}_2)/\sqrt{2}$ and $\vec{\phi}_B = (\vec{\phi}_1 - \vec{\phi}_2)/\sqrt{2}$,

$$L_q = \vec{\phi}_A \cdot \left[|\omega| + \left(1 - \frac{\gamma}{2}\right)q_x^2 + \left(1 + \frac{\gamma}{2}\right)q_y^2 + r \right]\vec{\phi}_A + \vec{\phi}_B \cdot \left[|\omega| + \left(1 + \frac{\gamma}{2}\right)q_x^2 + \left(1 - \frac{\gamma}{2}\right)q_y^2 + r \right]\vec{\phi}_B + L',$$

$$L' = A(|\vec{\phi}_A|^4 + |\vec{\phi}_B|^4) + B(\vec{\phi}_A \cdot \vec{\phi}_B)^2 + C|\vec{\phi}_A|^2|\vec{\phi}_B|^2. \quad (6)$$

After the redefinition, the Ising transformation becomes

$$x \to y, \quad y \to x,$$

$$\vec{\phi}_A \to \vec{\phi}_B, \quad \vec{\phi}_B \to -\vec{\phi}_A, \quad \sigma \to -\sigma. \quad (7)$$

Naively, all three quartic terms A, B, and C are marginal perturbations on the $z=2$ mean-field theory, a coupled renormalization-group (RG) equation is required to determine the ultimate fate of these terms. Notice that the anisotropy of the dispersion of $\vec{\phi}_A$ and $\vec{\phi}_B$ cannot be eliminated by redefining space and time; therefore, the number γ will enter the RG equation as a coefficient. The final coupled RG equation at the quadratic order for A, B, and C reads as

$$\frac{dA}{d\ln l} = -22A^2 - \frac{1}{2}B^2 - \frac{3}{2}C^2 - BC,$$

$$\frac{dB}{d\ln l} = -5uB^2 - 8AB - 8uBC,$$

$$\frac{dC}{d\ln l} = -uB^2 - 4AB - 20AC - 4uC^2. \quad (8)$$

u is a smooth function of γ, which decreases smoothly from $u=1$ in the isotropic limit with $\gamma=0$ to $u=0$ in the anisotropic limit with $\gamma=2$ (Fig. 3). With small γ, the function u can be expanded as $u = 1 - \gamma^2/12 - \gamma^4/120 + O(\gamma^6)$. The self-energy correction of $\vec{\phi}_a$ from the quartic terms will lead to the flow of the anisotropy ratio γ under RG, but the correction of this flow to the RG equation (8) is at even higher order.

The typical solution of the RG equation (8) is plotted in Fig. 4, for the most natural choice of the initial values of parameters with $\tilde{A} \gg \alpha$, $\tilde{A} \gg \tilde{C}$ in Eq. (4), i.e., the coupling between $\vec{\phi}_1$ and $\vec{\phi}_2$ is weak. One can see that the three parameters A, B, and C all have run-away flows and eventually become nonperturbative and likely drive the transition weakly first order. However, the three coefficients will first decrease and then increase under RG flow. This behavior implies that this run-away flow is extremely weak or, more precisely, even weaker than marginally relevant perturbations because marginally relevant operators will still monotonically increase under RG flow, although increases slowly. Therefore, in order to see this run-away flow, the correlation length has to be extremely long, i.e., the system has to be very close to the transition, so the transition remains one single second-order mean-field transition for a very large length and energy range. At the finite temperature quantum critical regime, the standard scaling arguments lead to the following scaling laws of physical quantities such as specific heat and the spin-lattice relaxation rate of NMR contributed by the quantum critical modes,[23]

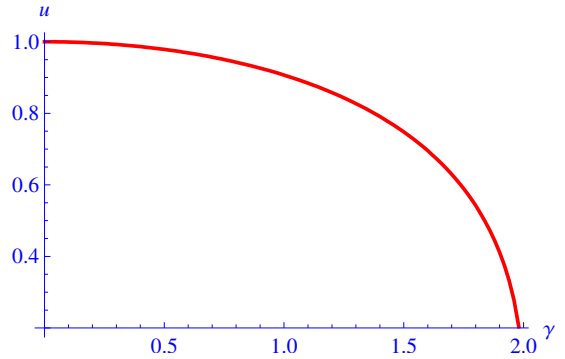

FIG. 3. (Color online) The plot of u in Eq. (8) against anisotropic dispersion coefficient γ between the isotropic limit $\gamma=0$ to anisotropic dispersion with $\gamma=1.95$.

$$C_v \sim T \ln\left(\frac{1}{T}\right), \quad \frac{1}{T_1} \sim \text{const}. \quad (9)$$

These scaling behaviors are obtained from ignoring the quartic perturbations. The quartic terms are marginal for a rather large energy scale (Fig. 4); therefore, to precisely calculate the physical quantities one should perform a perturbation

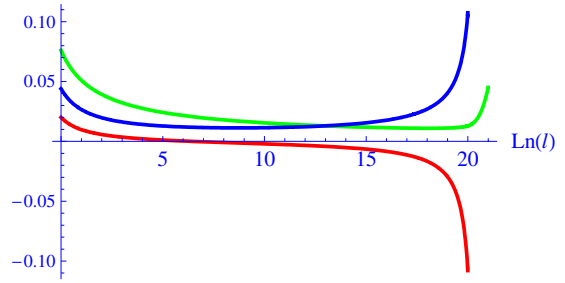

FIG. 4. (Color online) The solution of the RG equation (8). All three quartic perturbations decrease first then increase and finally become nonperturbative. The run-away flow is weaker than marginally relevant perturbations.

theory with constants A, B, and C, which may lead to further logarithmic corrections to the scaling laws.

The $\hat{z}$ direction tunneling of $\vec{\phi}_A$ and $\vec{\phi}_B$ between layers has so far been ignored, which is also a relevant perturbation at the $z=2$ mean-field fixed point. The $\hat{z}$ direction tunneling is written as $J_z \vec{\phi}_{a,z} \cdot \vec{\phi}_{a,z+1}$, which has scaling dimension 2 at the $z=2$, $d=2$ mean-field fixed point, and it becomes nonperturbative when

$$\frac{J_{in}}{J_z} \sim \left(\frac{\xi}{a}\right)^2 \sim r^{-1}. \tag{10}$$

This equation implies that if the tuning parameter r is in the small window $r < J_z/J_{in}$, the transition crossover back to a $z=2$, $d=3$ transition, where all the quartic perturbations A, B, and C are irrelevant. Since at the two-dimensional theory these quartic terms are only very weakly relevant, in the end the interlayer coupling J_z may win the race of the RG flow, and this transition becomes one stable mean-field second-order transition.

Now we have a global two-dimensional phase diagram, whose two axes are doping and pressure. The two second-order transition lines in the large doping and low-pressure side will merge to one single mean-field transition line in the low doping and high-pressure side of the phase diagram. Then inevitably there is a multicritical point where three lines merge together. At this multicritical point, the hole pockets will just touch the electron pocket after translating by wave vector $(\pi,0)$ [Fig. 2(c)]. Now the SDW order parameter $\vec{\phi}_A$ and $\vec{\phi}_B$ can still decay into particle-hole pairs, the Fermi's Golden rule and the lattice symmetry lead to the following overdamping term in the Lagrangian:

$$L_q = \left(\frac{|\omega|}{\sqrt{|q_x|}} + g\frac{|\omega|}{\sqrt{|q_y|}}\right)|\vec{\phi}_A|^2 + \left(g\frac{|\omega|}{\sqrt{|q_x|}} + \frac{|\omega|}{\sqrt{|q_y|}}\right)|\vec{\phi}_B|^2 + \cdots. \tag{11}$$

g is a constant, which is in general not unity because the system only enjoys the symmetry (7). The naive power counting shows that this field theory has dynamical exponent $z=5/2$, which makes all the quartic terms irrelevant. However, since the hole pockets and electron pockets are tangential after translating $(\pi,0)$, the expansion of the mean-field free energy in terms of the order parameters $\vec{\phi}_A$ and $\vec{\phi}_B$ contains a singular term $L_s \sim |\vec{\phi}_A|^{5/2} + |\vec{\phi}_B|^{5/2}$, which becomes very relevant at this naive $z=5/2$ fixed point. Similar singular term was found in the context of electronic nematic-smectic transition.[24] The existence of this singular term implies that, it is inadequate to start with a pure Bose theory by integrating out fermions, one should start with the Bose-Fermi mixed theory, with which perform the RG calculation. We will leave this sophisticated RG calculation to the future work; right now we assume this multicritical point is a special strongly interacting fixed point. The schematic three-dimensional global phase diagram is shown in Fig. 5.

In real system, due to the more complicated shape of the electron and hole pockets, with increasing doping the pockets will experience cutting and touching several times after translating by $(\pi,0)$ in the momentum space. We have used

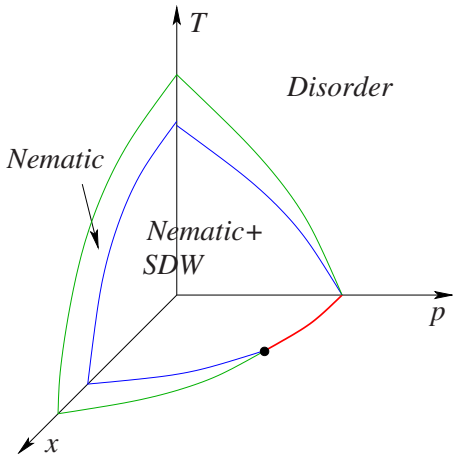

FIG. 5. (Color online) The global phase diagram of quasi-two-dimensional materials, with applications for 1111 materials. The finite temperature transition is always split to an Ising nematic transition and a SDW transition. The zero-temperature transitions depend on the doping and pressure. In the high doping and low-pressure side, the transition is split to two, as observed in experiments; in the low doping and high-pressure side, there is one single transition very close to the mean-field solution. A multicritical point, where the three transition lines merge is identified, which is expected to be a strongly coupled fixed point.

a five-band model developed in Ref. 25 with all the d orbitals on the Fe atoms and calculated the mean-field phase diagram close to the critical doping. The order parameter $\vec{\phi}_a$ couples to the electrons at the Fermi surface as $\Sigma_k \vec{\phi}_a \cdot c_k^\dagger \vec{\sigma} c_{k+\vec{Q}} + \text{H.c.}$ The mean-field energy of electrons due to nonzero spin order parameter $\vec{\phi}_a$ will renormalize r in field theory (6) and, hence, the critical r_c depends on the shape of the Fermi surface, which is tuned by doping. The critical r_c is expected to be proportional to the critical pressure p_c in the global phase diagram. r_c as a function of doping is plotted in Fig. 6, and the shapes of the Fermi pockets at the critical doping $x=7.6\%$ are plotted in Fig. 7.

The $z=2$ quantum critical behavior discussed in this section is only applicable to small enough energy scale. First of all, the damping term $|\omega|$ always competes with a quadratic term ω^2 in the Lagrangian, and at small enough energy scale the linear term dominates. If we assume the coupling between the spin order parameter $\vec{\phi}_a$ and the electrons is of the same order as the effective spin interaction J, the damping rate is linear with $\sim J^2\omega/E_f^2$, while the quadratic term is $\sim \omega^2/J$. Therefore, the frequency should be smaller than J^3/E_f^2 in order to apply the $z=2$ field theory (6). The value of J has been calculated by LDA (Ref. 26) and also measured with inelastic neutron scattering,[27] and both approaches indicate that $J \sim 50$ meV. E_f is the Fermi energy of the Fermi pockets, which is on the order of 200 meV. Therefore, the frequency-linear damping term will dominate the frequency quadratic term in the Lagrangian as long as $\omega < 3$ meV.

The damping rate of order parameters $\vec{\phi}_a$ is calculated assuming the Fermi surface can be linearly expanded close to the intersection point after translation in the momentum space; the criterion to apply this assumption depends on the details on the Fermi surface. In the particular situation under

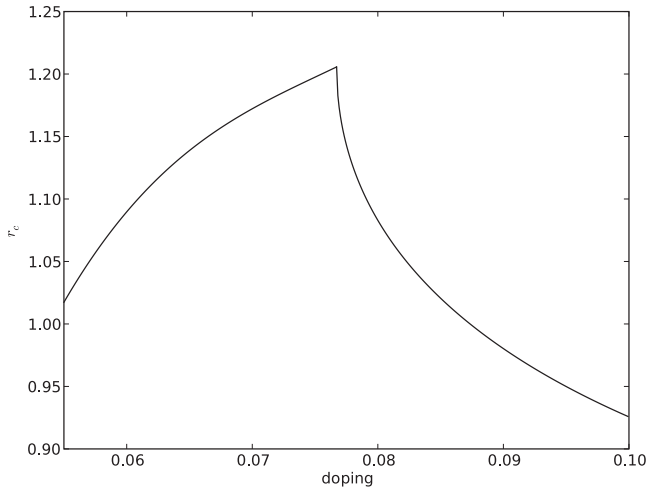

FIG. 6. Numerical results of r_c of $\vec{\phi}_a$ due to coupling to electrons. x axis is the electron doping. The peak of this curve corresponds to the critical doping x_c=7.6%, where electron and hole pockets touch each other after translating the hole pockets by the SDW wave vector. The two pockets intersect (separate) if doping is smaller (larger) than this critical doping. If $x>x_c$, the transition is split into two transitions by quantum fluctuations; if $x<x_c$, the transition is a z=2, d=2 transition with a very weak run-away flow in $2d$.

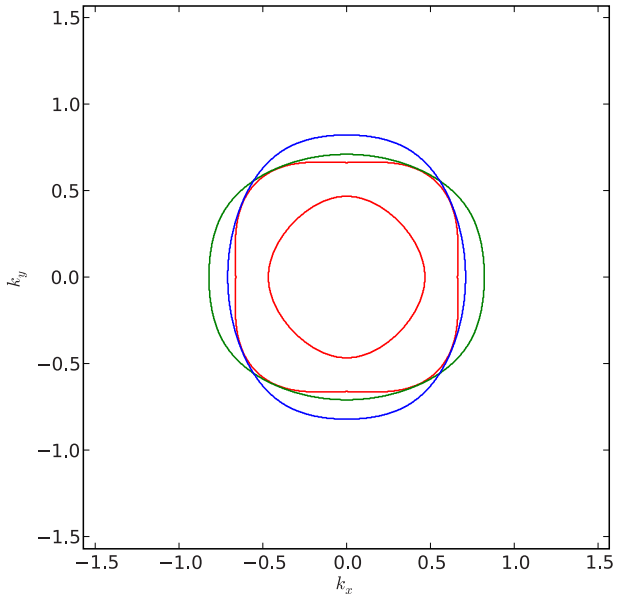

FIG. 7. (Color online) The plot of the hole and electron pockets after translating the hole pockets by the SDW wave vector, at the critical doping x=7.6%. The green circle is electron pocket located around $(0,\pi)$ and the blue one is electron pocket located around $(\pi,0)$.

discussion, this crossover energy scale is $\omega\sim 30$ meV in the undoped material, which is larger than the upper limit of 3 meV we obtained previously. Therefore, the ultraviolet cutoff of field theory (6) is estimated to be 3 meV.

III. THREE-DIMENSIONAL LATTICES

As mentioned in the introduction, compared with the 1111 materials, the 122 materials are much more isotropic, so we will treat this family of materials as a three-dimensional problem. If after translation by $(\pi,0)$ the hole pockets intersect with the electron pockets, the zero-temperature quantum transition is described a z=2, d=3 transition with analogous Lagrangian as Eq. (4), which becomes a stable mean-field transition. The finite temperature transition is described by two copies of coupled 3D O(3) transition. If the finite temperature transition is split into two transitions close to the quantum critical point, as observed in $BaFe_{2-x}Co_xAs_2$,[17] one can estimate the size of the splitting close to the quantum critical point. These two transitions, as explained before, are driven by the only relevant perturbation $\alpha(\vec{\phi}_1\cdot\vec{\phi}_2)^2$ at the coupled 3D O(3) transition because the Ising order parameter is obtained by minimizing this term through Hubbard-Stratonovich transformation. The scaling dimension of α at the 3D O(3) transition is $\Delta[\alpha]$=0.581, while α at the z=2, d=3 mean-field fixed point has dimension −1. Therefore, close to the quantum critical regime, to estimate the effect of α one should use the renormalized value $\alpha_R\sim\alpha\xi^{-1}\sim\alpha r^{1/2}$. The size of the splitting of the finite temperature transition close to the quantum critical point can be estimated as

$$\frac{\Delta T_c}{T_c}\sim\alpha_R^{1/(\nu\Delta[\alpha])}\sim\alpha^{1/(\nu\Delta[\alpha])}r^{1/(2\nu\Delta[\alpha])}. \tag{12}$$

ν is the exponent defined as $\xi\sim t^{-\nu}$ at the 3D O(3) universality class. T_c still scales with r in terms of a universal law $T_c\sim r^{z/(d-2+z)}$. The number α can be estimated in a J_1-J_2 Heisenberg model on the square lattice as introduced in Ref. 28; the value is given by $\alpha\sim J_1^2/J_2^2$. However, J_1-J_2 model is not designed for describing a metallic phase, so the legitimacy of applying the J_1-J_2 model to Fe pnictides is still under debate. In the finite temperature quantum critical regime, the specific heat, NMR relaxation rate $1/T_1$ scale as

$$C_v\sim T^{3/2},\quad \frac{1}{T_1}\sim T^{1/2}. \tag{13}$$

The similar analysis also applies when the finite temperature transition is one single first-order transition, which is the more common situation in 122 materials. One can estimate the jump of the lattice constant and the jump of the SDW order parameter at the finite temperature first-order transition close to the quantum critical point as

$$\delta\vec{\phi}_{sdw}\sim\alpha^{\beta/(\nu\Delta[\alpha])}r^{\beta/(2\nu\Delta[\alpha])},$$

$$\delta a\sim\alpha^{2\beta/(\nu\Delta[\alpha])}r^{\beta/(\nu\Delta[\alpha])}. \tag{14}$$

a is the lattice constant, which is linear with the Ising order parameter $\vec{\phi}_1\cdot\vec{\phi}_2$. β is the critical exponent at the 3D O(3) transition defined as $\langle\vec{\phi}_{sdw}\rangle\sim t^{\beta}$. However, it is difficult to determine whether there should be one first-order or two separate second-order transitions based on the relevance of parameter α, using universal formalism. An argument based on the dimensionality was given in the first section of this paper.

If under doping the hole pockets and electron pockets do not intersect (which depends on the details of $\hat{z}$ direction dispersions), this transition becomes two copies of coupled z=1, d=3 transition with three quartic terms A, B, and C,

$$L_q = \vec{\phi}_A \cdot \left[\omega^2 + \left(1 - \frac{\gamma}{2}\right) q_x^2 + \left(1 + \frac{\gamma}{2}\right) q_y^2 + q_z^2 + r \right] \vec{\phi}_A + \vec{\phi}_B \cdot \left[\omega^2 + \left(1 + \frac{\gamma}{2}\right) q_x^2 + \left(1 - \frac{\gamma}{2}\right) q_y^2 + q_z^2 + r \right] \vec{\phi}_B + L',$$

$$L' = A(|\vec{\phi}_A|^4 + |\vec{\phi}_B|^4) + B(\vec{\phi}_A \cdot \vec{\phi}_B)^2 + C|\vec{\phi}_A|^2 |\vec{\phi}_B|^2. \quad (15)$$

The coupled RG equation of the quartic terms is exactly the same as the one in Eq. (8); therefore, this free energy is also subjected to an extremely weak run-away flow, which is negligible unless the length scale is large enough. Again, one can estimate the universal scaling behavior in the quantum critical regime contributed by the quantum critical modes,

$$C_v \sim T^3, \quad \frac{1}{T_1} \sim T. \quad (16)$$

IV. COUPLING TO A SOFT LATTICE

Recent specific-heat measurement on $BaFe_{2-x}Co_xAs_2$ reveals two close but separate transitions at finite temperature, with a sharp peak at the SDW transition, and a discontinuity at the lattice distortion transition.[17] A discontinuity of specific heat is a signature of mean-field transition, in contrast to the sharp peak of Wilson-Fisher fixed point in a three-dimensional space. The specific-heat data suggest that the nature of the Ising nematic transition is strongly modified from the Wilson-Fisher fixed point, while SDW transition is unaffected. In the following, we will attribute this difference to the lattice strain field fluctuations.

The SDW transition at finite temperature should belong to the 3D O(3) transition if the lattice is ignored. The O(3) order parameter $\vec{\phi}$ couples to the lattice strain field with a quadratic term,[29]

$$|\vec{\phi}|^2(\partial_x u_x + \partial_y u_y + \lambda' \partial_z u_z), \quad (17)$$

which after integrating out the displacement vector generates a singular long-range interaction between $|\vec{\phi}|^2$ in the real space,

$$\int d^3r d^3r' g |\vec{\phi}|_r^2 \frac{f(\vec{r} - \vec{r}')}{|r - r'|^3} |\vec{\phi}|_{r'}^2. \quad (18)$$

f is a dimensionless function, which depends on the direction of $\vec{r} - \vec{r}'$. The scaling dimension of g is $\Delta[g] = \alpha = 2/\nu - 3$, and ν is the standard exponent at the 3D O(3) transition, which is greater than 2/3 according to various types of numerical computations.[20] Therefore, this long-range interaction is irrelevant at the 3D O(3) transition and, by coupling to the strain field of the lattice, the SDW transition is unaffected. However, if the SDW has an Ising uniaxial anisotropy, the SDW transition becomes a 3D Ising transition with $\nu < 2/3$, and the strain field would lead to a relevant long-range interaction.

However, since the symmetry of the Ising order parameter σ is the same as the shear strain of the lattice, the strain tensor will couple to the coarse-grained Ising field Φ as

$$F_{\Phi,\vec{u}} = \tilde{\lambda} \Phi(\partial_x u_y + \partial_y u_x) + \cdots. \quad (19)$$

$\vec{u}$ is the displacement vector. The ellipses are all the elastic modulus terms. Notice that we have rotated the coordinates by 45° since the true unit cell of the system is a two iron unit cell. After integrating out the displacement vector $\vec{u}$, the effective free energy of Φ gains a new singular term at small momentum,

$$F_{\theta,\phi} \sim f(\theta, \phi) |\Phi_k|^2. \quad (20)$$

f is a function of spherical coordinates θ and ϕ defined as $(k_x, k_y, k_z) = k[\cos(\theta)\cos(\phi), \cos(\theta)\sin(\phi), \sin(\theta)]$, but f is independent of the magnitude of momentum $\vec{k}$. By tuning the uniform susceptibility r, at some spherical angle of the space the minima of f start to condense, we will call these minima as nodal points. These nodal points are isolated from each other on the two-dimensional unit sphere labeled by the solid angles θ, ϕ and are distributed symmetrically on the unit sphere (θ, ϕ) according to the lattice symmetry transformation. Now suppose one nodal point of f is located at (θ_0, ϕ_0), we rotate the $\hat{z}$ direction along (θ_0, ϕ_0) and expand f at this nodal point in terms of $\tilde{\theta} = \theta - \theta_0$, the whole free energy can be written as

$$F = \int q^2 dq \tilde{\theta} d\tilde{\theta} (q^2 + \lambda \tilde{\theta}^2 + r) |\Phi_{q,\tilde{\theta}}|^2 + O(\Phi^4). \quad (21)$$

Notice that if $f(\theta_0, \phi_0)$ is a nodal point then $f(\pi - \theta_0, \pi + \phi_0)$ has to be another nodal point. The naive power counting shows that effectively the spatial dimension of this field theory (21) is $D = 5$, and the scaling dimension of $\Phi_{q,\theta}$ is $-7/2$. The quartic term Φ^4 takes an unusual form in the new momentum space of $q, \tilde{\theta}$, but the straightforward power counting indicates that it is still an irrelevant operator. Therefore, the strain tensor fluctuation effectively increases the dimension by two, which drives the transition a mean-field transition.

There is another way to formulate this effective five-dimensional theory. Let us rotate the $\hat{z}$ direction of the momentum space along the nodal point (θ_0, ϕ_0), then the scaling dimension of k_z is 1, and $k_x, k_y \sim k\tilde{\theta}$ effectively have scaling dimension 2. Therefore, expanded at the minimum the quadratic part of the free energy of Φ reads as

$$F = \int dk_x dk_y dk_z \left(\frac{k_x^2 + k_y^2}{k_z^2} + k_z^2 + r \right) |\Phi_k|^2 + \cdots. \quad (22)$$

The total dimension is still 5, considering $\Delta[k_x] = \Delta[k_y] = 2\Delta[k_z] = 2$. All the other momentum-dependent terms in the free energy are irrelevant.

The symmetry of the lattice allows multiple degenerate nodal points of function $f(\theta, \phi)$ on the unit sphere labeled by solid angles. If the only nodal points are north and south poles $\theta = 0, \pi$, which is allowed by the tetragonal symmetry of the lattice, the theory becomes a precise five-dimensional theory. However, the symmetry of the system also allows four stable degenerate nodal points on the equator, for instance, at $(\pi/2, n\pi/2)$ with $n = 0 \sim 3$. Close to nodal points $n = 0, 2$, $\Delta[k_z] = \Delta[k_y] = 2\Delta[k_x] = 2$, while close to nodal points

$n=1,3$, $\Delta[k_z]=\Delta[k_x]=2\Delta[k_y]=2$. Therefore, the scattering between these nodal points complicates the naive counting of the scaling dimensions, although $\Delta[k_z]=2$ is still valid. The transition in this case may still be a stable mean-field transition, but a more careful analysis of the loop diagrams is demanded to be certain. Let us denote the Φ mode at $(\pi/2,0)$ and $(\pi/2,\pi)$ as Φ_1 and Φ_1^* and denote $(\pi/2,\pi/2)$ and $(\pi/2,-\pi/2)$ modes as Φ_2 and Φ_2^*, the expanded free energy reads as

$$
\begin{aligned}
F = \int dk_x dk_y dk_z \left(\frac{k_z^2+k_y^2}{k_x^2} + k_x^2 + r \right) |\Phi_{1,k}|^2 + \left(\frac{k_z^2+k_x^2}{k_y^2} + k_y^2 + r \right) \\
\times |\Phi_{2,k}|^2 + \sum_{a=1}^{2} \delta\left(\sum_{i=1}^{4} \vec{k}_i \right) g \Phi_{a,k_1} \Phi_{a,k_2} \Phi_{a,k_3} \Phi_{a,k_4} \\
+ \delta\left(\sum_{i=1}^{4} \vec{k}_i \right) g_1 \Phi_{1,k_1} \Phi_{1,k_2} \Phi_{2,k_3} \Phi_{2,k_4} \\
+ \delta\left(\sum_{i=1}^{4} \vec{k}_i \right) g_2 \Phi_{1,k_1} \Phi_{2,k_2} \Phi_{2,k_3} \Phi_{2,k_4} \\
+ \delta\left(\sum_{i=1}^{4} \vec{k}_i \right) g_2 \Phi_{1,k_1} \Phi_{1,k_2} \Phi_{1,k_3} \Phi_{2,k_4}. \qquad (23)
\end{aligned}
$$

The g_1 and g_2 terms describe the scattering between different nodal points. To see whether the mean-field transition is stable, one can calculate the one-loop corrections to g_1 and g_2. The result is that none of the loops introduces nonperturbative divergence in the infrared limit, i.e., the quartic terms remain perturbative at the mean-field fixed point. This analysis suggests that the Ising nematic transition is a mean-field transition even with multiple nodal points of function $f(\theta,\phi)$ on the equator.

V. SUMMARIES AND EXTENSIONS

In this work, we studied the global phase diagram of the magnetic order and lattice distortion of the Fe-pnictides superconductors. Two-dimensional and three-dimensional formalisms were used for 1111 and 122 materials, respectively. The superconductivity was ignored so far in this material. If the quantum critical points discussed in this paper occur inside the superconducting phase, our results can be applied to the case when superconducting phase is suppressed. For instance, in 1111 materials, if a transverse magnetic field higher than $H_{c2,ab}$ is turned on, the field theories (2) and (6) become applicable. If the T_c of the superconductor is lower than the ultraviolet cutoff of our field theory, the scaling behavior predicted in our work can be applied to the temperature between T_c and the cutoff. Inside the superconducting phase, the nature of the transition may be changed. In 122 materials, the angle resolved photoemission spectroscopy measurements on single crystals indicate that the Fermi pockets are fully gapped in the superconducting phase;[30] therefore, the magnetic and nematic transitions are described by the $z=1$, $d=3$ field theory (15), which is an extremely weak first-order transition. In 1111 materials, although many experimental facts support a fully gapped Fermi surface, d-wave pairing with nodal points is still favored by the Andreev reflection measurements.[31,32] The nematic transition in the background of d-wave superconductor is studied in Refs. 33–35.

In most recently discovered 11 materials $Fe_{1+y}Se_xTe_{1-x}$, the SDW and lattice distortion are both different from the 1111 and 122 materials.[10] The SDW state breaks the reflection symmetries about both $x=y$ line and $\hat{x}$ axis, i.e., there are two different Ising symmetries broken in the SDW state, the ground-state manifold is $S^2\times Z_2\times Z_2$. In this case, the classical and quantum phase diagrams are more interesting and richer and, since the order moments of the SDW in 11 materials are much larger than 1111 and 122 materials (about $2\mu_B$), a lattice Heisenberg model with nearest-neighbor, second-nearest-neighbor, and third-nearest-neighbor interactions (J_1-J_2-J_3) may be adequate in describing 11 materials, as was studied in Ref. 36.

Besides the quantum phase transitions studied in our current work, a quantum critical point is conjectured between the P-based and As-based materials,[37] the field theory of this quantum critical point is analogous to Eq. (4). The formalism used in our work is also applicable to phase transitions in other strongly correlated materials, for instance, the spin-dimer material $BaCuSi_2O_6$, which under strong magnetic field develops long-range XY order interpreted as condensation of spin triplet component $S^z=-1$.[38] This quantum critical point also has dynamical exponent $z=2$, although the frequency-linear term is from the Larmor precession induced by the magnetic field, instead of damping with particle-hole excitations. The frustration between the nearest-neighbor layers in this material introduces an extra Ising symmetry between the even and odd layers besides the XY spin symmetry; therefore, the quartic terms of this field theory are identical with Eq. (6). The RG equations of these quartic terms are much simpler than Eq. (8) because only the "ladderlike" Feynman diagrams need to be taken into account.[39] We will study the material $BaCuSi_2O_6$ in detail in a future work.[40]

ACKNOWLEDGMENTS

We thank Subir Sachdev and Qimiao Si for helpful discussions. We especially appreciate Bert Halperin for educating us about his early work on phase transitions on soft cubic lattice.[29]

[1] Clarina de la Cruz, Q. Huang, J. W. Lynn, J. Li, W. Ratcliff II, J. L. Zarestky, H. A. Mook, G. F. Chen, J. L. Luo, N. L. Wang, and P. Dai, Nature (London) **453**, 899 (2008).
[2] C. Xu, M. Muller, and S. Sachdev, Phys. Rev. B **78**, 020501(R) (2008).
[3] C. Fang, H. Yao, W.-F. Tsai, J. P. Hu, and S. A. Kivelson, Phys. Rev. B **77**, 224509 (2008).
[4] M. A. McGuire, A. D. Christianson, A. S. Sefat, B. C. Sales, M. D. Lumsden, R. Jin, E. A. Payzant, D. Mandrus, Y. Luan, V. Keppens, V. Varadarajan, J. W. Brill, R. P. Hermann, M. T. Sougrati, F. Grandjean, and G. J. Long, Phys. Rev. B **78**, 094517 (2008).
[5] Q. Huang, Y. Qiu, W. Bao, M. A. Green, J. W. Lynn, Y. C. Gasparovic, T. Wu, G. Wu, and X. H. Chen, Phys. Rev. Lett. **101**, 257003 (2008).
[6] C. Krellner, N. Caroca-Canales, A. Jesche, H. Rosner, A. Ormeci, and C. Geibel, Phys. Rev. B **78**, 100504(R) (2008).
[7] J.-Q. Yan, A. Kreyssig, S. Nandi, N. Ni, S. L. Bud'ko, A. Kracher, R. J. McQueeney, R. W. McCallum, T. A. Lograsso, A. I. Goldman, and P. C. Canfield, Phys. Rev. B **78**, 024516 (2008).
[8] J. Zhao, W. Ratcliff II, J. W. Lynn, G. F. Chen, J. L. Luo, N. L. Wang, J. Hu, and P. Dai, Phys. Rev. B **78**, 140504(R) (2008).
[9] A. I. Goldman, D. N. Argyriou, B. Ouladdiaf, T. Chatterji, A. Kreyssig, S. Nandi, N. Ni, S. L. Bud'ko, P. C. Canfield, and R. J. McQueeney, Phys. Rev. B **78**, 100506(R) (2008).
[10] S. Li, Clarina de la Cruz, Q. Huang, Y. Chen, J. W. Lynn, J. Hu, Y.-L. Huang, F.-C. Hsu, K.-W. Yeh, M.-K. Wu, and P. Dai, Phys. Rev. B **79**, 054503 (2009).
[11] P. Chandra, P. Coleman, and A. I. Larkin, Phys. Rev. Lett. **64**, 88 (1990).
[12] F. Ma, Z. Lu, and T. Xiang, arXiv:0806.3526 (unpublished).
[13] H. Q. Yuan, J. Singleton, F. F. Balakirev, G. F. Chen, J. L. Luo, and N. L. Wang, Nature (London) **457**, 565 (2009).
[14] J. Zhao, Q. Huang, Clarina de la Cruz, S. Li, J. W. Lynn, Y. Chen, M. A. Green, G. F. Chen, G. Li, Z. Li, J. L. Luo, N. L. Wang, and P. Dai, Nature Mater. **7**, 953 (2008).
[15] R. H. Liu, G. Wu, T. Wu, D. F. Fang, H. Chen, S. Y. Li, K. Liu, Y. L. Xie, X. F. Wang, R. L. Yang, L. Ding, C. He, D. L. Feng, and X. H. Chen, Phys. Rev. Lett. **101**, 087001 (2008).
[16] S. Margadonna, Y. Takabayashi, M. T. McDonald, M. Brunelli, G. Wu, R. H. Liu, X. H. Chen, and K. Prassides, Phys. Rev. B **79**, 014503 (2009).
[17] J.-H. Chu, J. G. Analytis, C. Kucharczyk, and I. R. Fisher, Phys. Rev. B **79**, 014506 (2009).
[18] N. Ni, M. E. Tillman, J.-Q. Yan, A. Kracher, S. T. Hannahs, S. L. Bud'ko, and P. C. Canfield, Phys. Rev. B **78**, 214515 (2008).
[19] F. L. Ning, K. Ahilan, T. Imai, A. S. Sefat, R. Jin, M. A. McGuire, B. C. Sales, and D. Mandrus, J. Phys. Soc. Jpn. **78**, 013711 (2009).
[20] P. Calabrese, A. Pelissetto, and E. Vicari, arXiv:cond-mat/0306273 (unpublished).
[21] J. A. Hertz, Phys. Rev. B **14**, 1165 (1976).
[22] V. Oganesyan, S. A. Kivelson, and E. Fradkin, Phys. Rev. B **64**, 195109 (2001).
[23] L. Zhu, M. Garst, A. Rosch, and Q. Si, Phys. Rev. Lett. **91**, 066404 (2003).
[24] K. Sun, B. M. Fregoso, M. J. Lawler, and E. Fradkin, Phys. Rev. B **78**, 085124 (2008).
[25] K. Kuroki, S. Onari, R. Arita, H. Usui, Y. Tanaka, H. Kontani, and H. Aoki, Phys. Rev. Lett. **101**, 087004 (2008).
[26] F. Ma, Z. Y. Lu, and T. Xiang, Phys. Rev. B **78**, 224517 (2008).
[27] J. Zhao, D.-X. Yao, S. Li, T. Hong, Y. Chen, S. Chang, W. Ratcliff II, J. W. Lynn, H. A. Mook, G. F. Chen, J. L. Luo, N. L. Wang, E. W. Carlson, J. Hu, and P. Dai, Phys. Rev. Lett. **101**, 167203 (2008).
[28] Q. Si and E. Abrahams, Phys. Rev. Lett. **101**, 076401 (2008).
[29] D. Bergman and B. I. Halperin, Phys. Rev. B **13**, 2145 (1976).
[30] H. Ding, P. Richard, K. Nakayama, T. Sugawara, T. Arakane, Y. Sekiba, A. Takayama, S. Souma, T. Sato, T. Takahashi, Z. Wang, X. Dai, Z. Fang, G. F. Chen, J. L. Luo, and N. L. Wang, EPL **83**, 47001 (2008).
[31] O. Millo, I. Asulin, O. Yuli, I. Felner, Z.-A. Ren, X.-L. Shen, G.-C. Che, and Z.-X. Zhao, Phys. Rev. B **78**, 092505 (2008).
[32] Y. Wang, L. Shan, L. Fang, P. Cheng, C. Ren, and H.-H. Wen, Supercond. Sci. Technol. **22**, 015018 (2009).
[33] E.-A. Kim, M. J. Lawler, P. Oreto, S. Sachdev, E. Fradkin, and S. A. Kivelson, Phys. Rev. B **77**, 184514 (2008).
[34] C. Xu, Y. Qi, and S. Sachdev, Phys. Rev. B **78**, 134507 (2008).
[35] Y. Huh and S. Sachdev, Phys. Rev. B **78**, 064512 (2008).
[36] B. Chen Fang, A. Bernevig, and J. Hu, EPL **86**, 67006 (2009).
[37] J. Dai, Q. Si, J. Zhu, and E. Abrahams, Proc. Natl. Acad. Sci. U.S.A. **106**, 4118 (2009).
[38] S. E. Sebastian, N. Harrison, C. D. Batista, L. Balicas, M. Jaime, P. A. Sharma, N. Kawashima, and I. R. Fisher, Nature (London) **441**, 617 (2006).
[39] S. Sachdev, *Quantum Phase Transitions* (Cambridge University Press, Cambridge, 1998).
[40] C. Xu (unpublished).